# Improving iterative 4D CBCT through the use of motion information

Cyril Mory, Simon Rit

***Abstract*—In Image-Guided RadioTherapy (IGRT) of lung tumors, patients undergo a 4D CT, on the basis of which their treatment is planned. It is implicitely assumed that their breathing motion will not change much throughout the treatment, and remain close to what it was during the 4D CT acquisition. During the treatment, several cone beam CT acquisitions are performed, and used to re-position the patient. Obtaining a 4D reconstruction from this cone beam data would allow the therapists to check whether the breathing motion of the day still matches that of the planning CT, and if not, take appropriate corrective actions. Unfortunately, most tomography methods currently available are inadequate for such a task: static 3D reconstructions are pointless for motion assessment, respiration-correlated reconstructions are affected by streak artifacts, and regularization techniques only bring limited improvement. Recently, regularized 4D methods have been proposed, in which the whole respiratory cycle is reconstructed at once. As these methods allow to explicitely enforce similarity between consecutive frames, they considerably improve image quality. In the case of IGRT, the motion information extracted from the 4D planning CT can be used to further improve the 4D reconstruction results. We describe a recent 4D reconstruction method (ROOSTER), propose its motion-compensated counterpart (MC-ROOSTER), and compare their results.**

## I. Introduction

In image-guided radiotherapy (IGRT) of lung tumors, breathing motion affects the image guidance. On a treatment day, physicians currently have no reliable method to verify that the patient's breathing motion is the same as in the planning CT. This task requires a 4D reconstruction of the cone beam CT data, but most reconstruction methods currently available suffer major drawbacks: static reconstruction techniques, like FDK [1] or SART [2], generate images almost free of streaks, but in 3D, not 4D, and in which the moving structures are strongly blurred. Their respiration-correlated counterparts generate severely degraded 4D images with strong streak artifacts, unless the acquisition time is substantially increased [3]. Advanced methods have been developed to achieve streak-free and blur-free 4D reconstructions, most of which are either based on motion compensation [4], [5], [6], [7], [8], some of which are currently in use in hospitals, or on regularization using some a priori information [9], [10], [11], [12], [13], [14], [15], [16], [17]. Recently, mixed methods have been proposed, which combine both approaches [18]. We describe a recent 4D reconstruction method (ROOSTER) [17], propose its motion-compensated counterpart (MC-ROOSTER), and compare their results.

C. Mory works for the iMagX project, ICTEAM Institute, Université catholique de Louvain, Louvain-la-Neuve, Belgium and the Université de Lyon, CREATIS ; CNRS UMR5220 ; Inserm U1044 ; INSA-Lyon ; Université Lyon 1 ; Centre Léon Bérard, France e-mail: cyril.mory@creatis.insa-lyon.fr.

S. Rit works for the Université de Lyon, CREATIS ; CNRS UMR5220 ; Inserm U1044 ; INSA-Lyon ; Université Lyon 1 ; Centre Léon Bérard, France.

iMagX is a public partnership between UCL and IBA funded by the Walloon region under convention number 1017266 and 1217662.

## II. Original ROOSTER method

The ROOSTER algorithm assumes that a rough segmentation of the patient is available, and that movement is expected to occur only inside this segmented region. The method consists in iteratively enforcing five different constraints in an alternating manner. It starts by minimizing a quadratic data-attachment term $\sum_{\alpha} \|R_\alpha S_\alpha f - p_\alpha\|_2^2$, with $\alpha$ the projection's index, $f$ a 4D sequence of volumes, $R_\alpha$ the forward projection operator for the projection with index $\alpha$, $S_\alpha$ a linear interpolator which, from the 4D sequence $f$, estimates the 3D volume through which projection $\alpha$ has been acquired, and $p_\alpha$ the measured projection with index $\alpha$. This data-attachment term is minimized by conjugate gradient. Then the following regularization steps are applied sequentially: positivity enforcement, averaging along time outside the segmentation, spatial total-variation denoising, and temporal total-variation denoising. By spatial and temporal TV denoising, we mean finding $f_{Space} = \arg\min_f \|f - f_{Averaged}\|_2^2 + \gamma_{Space} TV_{Space}(f)$ and $f_{Time} = \arg\min_f \|f - f_{Space}\|_2^2 + \gamma_{Time} TV_{Time}(f)$ respectively. It boils down to finding the proximal operator of $TV$, which fortunately is a well-studied problem [19]. This constitutes one iteration of the main loop, the output of which is fed back to the conjugate gradient minimizer for the next iteration.

ROOSTER requires only two parameters, the aforementionned $\gamma_{Space}$ and $\gamma_{Time}$, which control the amount of regularization by balancing the $TV$ and data-attachment terms in the denoising cost functions. The optimal values of these parameters depend on the size and spacing of $f$, on its mean intensity and the way it varies in space and time, and on the aspect one whishes to obtain on the denoised image. They are found empirically, but do not have to be patient-specific: once satisfactory values of $\gamma_{Space}$ and $\gamma_{Time}$ have been obtained for one patient, they can be used for the others.

The temporal total variation denoising step enforces similarity between consecutive frames, efficiently removing streak artifacts. However, when structures undergo high amplitude movements, this step ends up enforcing similarity between unrelated structures, removing the faintest ones and blurring the borders of the larger ones.

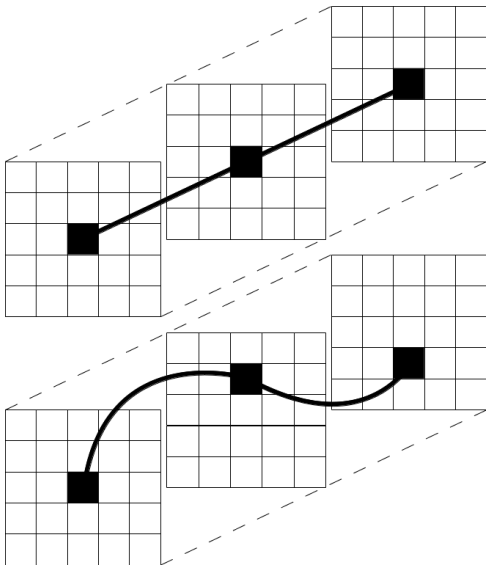

Fig. 1. Possible trajectories for denoising along time. On top, constant $(x, y, z)$, as used by ROOSTER. At the bottom, curved trajectory taking estimated motion into account, as used by MC-ROOSTER.

## III. Motion-Compensated ROOSTER

In IGRT, some motion information can be estimated from the planning CT (and is already, in some cancer treatment centers). This information is, for example, used to perform a motion-compensated FDK reconstruction [4]. Here, we propose to use it in a different fashion: we modify the temporal total variation denoising step of ROOSTER to operate along a curved trajectory, following the estimated motion of each voxel along time, instead of along a fixed $(x, y, z)$ trajectory. This is illustrated in figure 1.

The step-by-step description of this regularization along a curved trajectory is as follows:

- Each frame is warped to a reference position using the estimated motion. This warping is performed by trilinear interpolation (called inverse mapping, in [20]). Let $W$ be the trilinear interpolation warping operator.
- 1D-TV denoising is applied along time on the warped volumes. Let $D_{time}$ be the total variation denoising along time operator. Note that unlike $W$, $D_{time}$ is not a linear operator.
- Each denoised frame is then warped back to its original position, by applying $W^{-1}$

Unfortunately, we have found no simple way to compute $W^{-1}$ with a sufficiently high precision. Using a low-precision approximation of $W^{-1}$ causes some regularization artifacts to accumulate over the iterations, and MC-ROOSTER as a whole to diverge. The solution we propose is to seek a least-squares approximation of $f_{Denoised} = W^{-1} D_{time}(W f_{Space})$. It amounts to solving

$$f_{Denoised} = \arg\min_f \|Wf - D_{time}(W f_{Space})\|_2^2 \quad (1)$$

The minimum is reached when the gradient of the L2 norm is null, i.e. when

$$W^T W f = W^T D_{time}(W f_{Space}) \quad (2)$$

where $W^T$ is the adjoint of the trilinear interpolation operator, i.e. the normalized trilinear splat operator (called Forward mapping in [20]). We solve this problem by conjugate gradient. Although it is image-dependent, this method provides a sufficiently precise inversion of $W$, and regularization artifacts do not appear.

Note that MC-ROOSTER with a zero-amplitude estimated motion is equivalent to ROOSTER. Therefore, as soon as the estimated motion is better than a zero-amplitude motion (i.e. closer to the real motion), MC-ROOSTER can be expected to yield better reconstruction results than ROOSTER. MC-ROOSTER requires the same two parameters as ROOSTER.

## IV. Results

A CBCT acquisition performed on a patient was reconstructed with static 3D FDK, respiration-correlated 4D FDK, ROOSTER and MC-ROOSTER. The 4D DVF was estimated on a prior 4D planning CT using a method that allows sliding motion at the border between the lungs and the chest wall [21], [22]. The size of the reconstructed sequence of volumes was set to $145 \times 185 \times 245$ voxels, with isotropic voxels of size 1.5 mm in each dimension. Both ROOSTER and MC ROOSTER reconstruct the respiratory cycle as a sequence of 10 such volumes.

Figure 2 shows a sagittal slice of the reconstructions obtained using four different methods, and Figure 3 the coronal slice.

The static FDK reconstruction is blurry, and small structures in the lungs are blurred out. The contours of the tumor cannot be delineated. The respiration-correlated FDK reconstructions exhibit high intensity streak artifacts, which here appear as dark and bright areas as the cut planes intersect the streaks (they would appear line-shaped in transverse view). In ROOSTER reconstructions, especially at end-inhale, many small structures are wiped away by the temporal regularization. In the MC-ROOSTER reconstructions, on the other hand, they are visible and can be delineated. Furthermore, viewing the 4D reconstructions as movies shows structures gradually fading in the ROOSTER reconstructions, while they have sharp motion and distinct borders throughout the breathing cycle with MC-ROOSTER.

## V. Discussion

In the case presented here, the motion estimation obtained on the 4D planning CT is very precise, which explains the large gain in image quality. Note that when a precise motion estimation is indeed available, a simple motion-compensated FDK (MC-FDK) also provides a high image quality. However, as one of the goals is to verify that the motion of the treatment day is similar to that of the planning CT, an MC-FDK is pointless. The main point we wish to make in this paper is that a major increase in image quality can be obtained by modifying only the regularization along time and making it work along (relevant) curved trajectories. This behavior can be

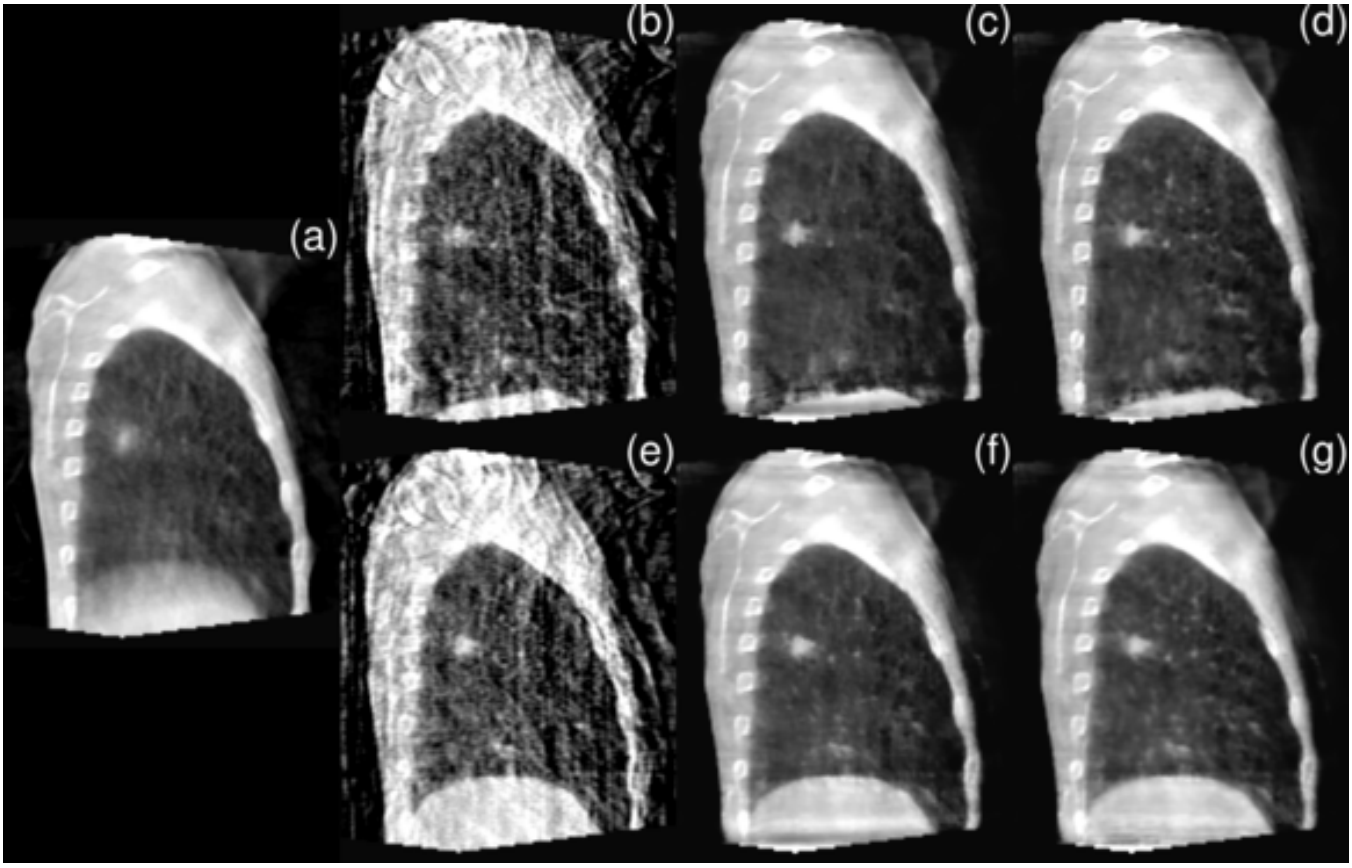


Fig. 2. Sagittal slice of a patient with lung tumor (a) Static FDK (b) Respiration-correlated FDK, end-inhale (c) ROOSTER, end-inhale (d) MC-ROOSTER, end-inhale (e) Respiration-correlated FDK, end-exhale (f) ROOSTER, end-exhale (g) MC-ROOSTER, end-exhale

obtained by inputing motion information, as we have proved it, but other methods (e.g. block matching techniques or Temporal Non-Local Means (TNLM) [14]) should also be considered. When no information on motion is available a-priori, these alternative methods would probably yield results superior to those of ROOSTER. When some motion estimation can be obtained, it can be used to run MC-ROOSTER, but it could also serve as initialization for the search of similar blocks in TNLM.

In order to become usable in clinical practice, MC-ROOSTER would need to achieve computation times below one minute. On an Intel Xeon E5-2620 CPU with 12 cores, equipped with an nVidia GTX780 GPU, running OpenSuse 13.1 and The Reconstruction ToolKit (RTK) [23], it currently takes about one minute to perform a single iteration of the main loop, and the results presented in this paper have been obtained with 10 iterations. The most time-consuming part in MC-ROOSTER is the conjugate gradient optimization on the data fidelity term, which requires multiple forward and back projections of the whole dataset. Replacing this part with a 4D version of OS-SART [24], [25] could bring a noticeable speed up. Whether satisfactory computation times can then be achieved by code optimization remains a question.

## REFERENCES

[1] L. A. Feldkamp, L. C. Davis, and J. W. Kress, "Practical cone-beam algorithm," *Journal of the Optical Society of America A*, vol. 1, no. 6, pp. 612–619, Jun. 1984.

[2] A. H. Andersen and A. C. Kak, "Simultaneous algebraic reconstruction technique (SART): a superior implementation of the art algorithm," *Ultrasonic Imaging*, vol. 6, no. 1, pp. 81–94, Jan. 1984.

[3] J.-J. Sonke, L. Zijp, P. Remeijer, and M. van Herk, "Respiratory correlated cone beam CT," *Medical Physics*, vol. 32, no. 4, p. 1176, 2005.

[4] S. Rit, J. W. H. Wolthaus, M. van Herk, and J.-J. Sonke, "On-the-fly motion-compensated cone-beam CT using an a priori model of the respiratory motion," *Medical physics*, vol. 36, no. 6, pp. 2283–2296, Jun. 2009.

[5] S. Rit, D. Sarrut, and L. Desbat, "Comparison of analytic and algebraic methods for motion-compensated cone-beam CT reconstruction of the thorax," *IEEE Transactions on Medical Imaging*, vol. 28, no. 10, pp. 1513–1525, Oct. 2009.

[6] S. Rit, J. Nijkamp, M. van Herk, and J.-J. Sonke, "Comparative study of respiratory motion correction techniques in cone-beam computed tomography," *Radiotherapy and Oncology*, vol. 100, no. 3, pp. 356–359, Sep. 2011.

[7] M. Brehm, P. Paysan, M. Oelhafen, P. Kunz, and M. Kachelrie, "Self-adapting cyclic registration for motion-compensated cone-beam CT in image-guided radiation therapy," *Medical Physics*, vol. 39, no. 12, pp. 7603–7618, Dec. 2012.

[8] J. Wang and X. Gu, "High-quality four-dimensional cone-beam CT by deforming prior images," *Physics in Medicine and Biology*, vol. 58, no. 2, p. 231, Jan. 2013.

[9] S. Leng, J. Tang, J. Zambelli, B. Nett, R. Tolakanahalli, and G.-H. Chen, "High temporal resolution and streak-free four-dimensional cone-beam computed tomography," *Physics in medicine and biology*, vol. 53, no. 20, pp. 5653–5673, Oct. 2008.

[10] E. Y. Sidky and X. Pan, "Image reconstruction in circular cone-beam computed tomography by constrained, total-variation minimization," *Physics in Medicine and Biology*, vol. 53, no. 17, pp. 4777–4807, Sep. 2008.

[11] F. Bergner, T. Berkus, M. Oelhafen, P. Kunz, T. Pan, R. Grimmer,

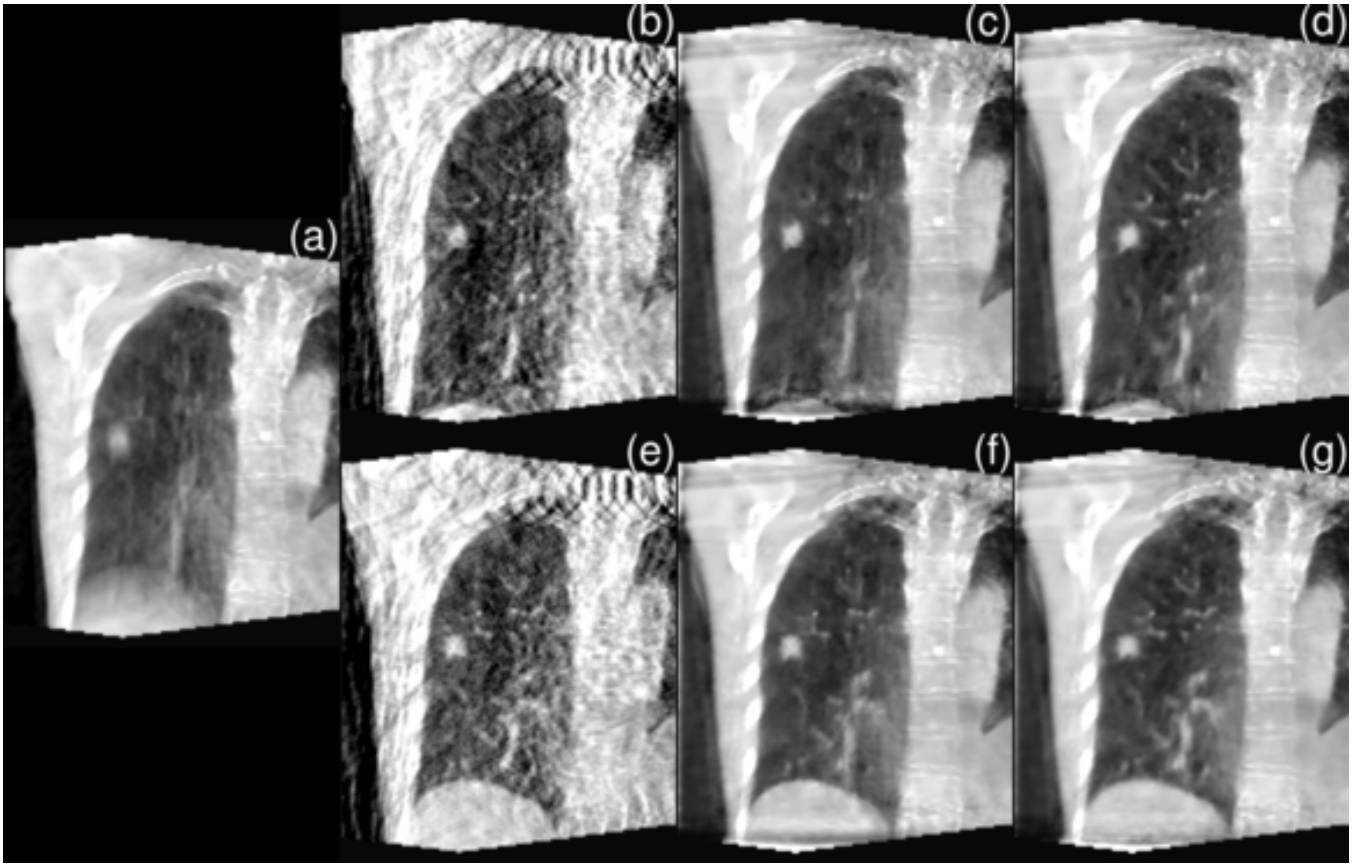


Fig. 3. Coronal slice of a patient with lung tumor(a) Static FDK (b) Respiration-correlated FDK, end-inhale (c) ROOSTER, end-inhale (d) MC-ROOSTER, end-inhale (e) Respiration-correlated FDK, end-exhale (f) ROOSTER, end-exhale (g) MC-ROOSTER, end-exhale

L. Ritschl, and M. Kachelrie, "An investigation of 4d cone-beam CT algorithms for slowly rotating scanners," *Medical Physics*, vol. 37, no. 9, p. 5044, 2010.

[12] X. Jia, Y. Lou, B. Dong, Z. Tian, and S. Jiang, "4d computed tomography reconstruction from few-projection data via temporal non-local regularization," in *Medical Image Computing and Computer-Assisted Intervention MICCAI 2010*, ser. Lecture Notes in Computer Science, T. Jiang, N. Navab, J. P. W. Pluim, and M. A. Viergever, Eds. Springer Berlin Heidelberg, Jan. 2010, no. 6361, pp. 143–150.

[13] Z. Qi and G.-H. Chen, "Extraction of tumor motion trajectories using PICCS-4dcbct: a validation study," *Medical physics*, vol. 38, no. 10, pp. 5530–5538, Oct. 2011.

[14] Z. Tian, X. Jia, B. Dong, Y. Lou, and S. B. Jiang, "Low-dose 4dct reconstruction via temporal nonlocal means," *Medical physics*, vol. 38, no. 3, pp. 1359–1365, Mar. 2011.

[15] H. Gao, R. Li, Y. Lin, and L. Xing, "4d cone beam CT via spatiotemporal tensor framelet," *Medical Physics*, vol. 39, no. 11, pp. 6943–6946, Nov. 2012.

[16] H. Wu, A. Maier, R. Fahrig, and J. Hornegger, "Spatial-temporal total variation regularization (STTVR) for 4d-CT reconstruction," in *Proceedings of SPIE Medical Imaging 2012*, N. J. Pelc, R. M. Nishikawa, and B. R. Whiting, Eds., San Diego, CA, USA, Feb. 2012, p. 83133J.

[17] C. Mory, V. Auvray, B. Zhang, M. Grass, D. Schfer, S. J. Chen, J. D. Carroll, S. Rit, F. Peyrin, P. Douek, and L. Boussel, "Cardiac c-arm computed tomography using a 3d + time ROI reconstruction method with spatial and temporal regularization," *Medical physics*, vol. 41, no. 2, p. 021903, Feb. 2014.

[18] J. Wang and X. Gu, "Simultaneous motion estimation and image reconstruction (SMEIR) for 4d cone-beam CT," *Medical Physics*, vol. 40, no. 10, p. 101912, Oct. 2013.

[19] A. Chambolle, "An algorithm for total variation minimization and applications," *J. Math. Imaging Vis.*, vol. 20, no. 1-2, pp. 89–97, Jan. 2004.

[20] G. Wolberg, *Digital Image Warping*. Los Alamitos, Calif: Wiley-Blackwell, 1990.

[21] J. Vandemeulebroucke, S. Rit, J. Kybic, P. Clarysse, and D. Sarrut, "Spatiotemporal motion estimation for respiratory-correlated imaging of the lungs," *Medical physics*, vol. 38, no. 1, pp. 166–178, Jan. 2011.

[22] V. Delmon, S. Rit, R. Pinho, and D. Sarrut, "Registration of sliding objects using direction dependent b-splines decomposition," *Physics in Medicine and Biology*, vol. 58, no. 5, p. 1303, Mar. 2013.

[23] S. Rit, M. Vila Oliva, S. Broumische, R. Labarbe, D. Sarrut, and G. C. Sharp, "The reconstruction toolkit (RTK), an open-source cone-beam CT reconstruction toolkit based on the insight toolkit (ITK)," in *Proceedings of the International Conference on the Use of Computers in Radiation Therapy (ICCR)*, 2013.

[24] G. Wang and M. Jiang, "Ordered-subset simultaneous algebraic reconstruction techniques (OS-SART)," *Journal of X-Ray Science and Technology*, vol. 12, no. 3, pp. 169–177, Jan. 2004.

[25] F. Xu, W. Xu, M. Jones, B. Keszthelyi, J. Sedat, D. Agard, and K. Mueller, "On the efficiency of iterative ordered subset reconstruction algorithms for acceleration on GPUs," *Computer methods and programs in biomedicine*, vol. 98, no. 3, pp. 261–270, Jun. 2010.